DELAMINATION/DEBOND GROWTH IN Z-FIBRE REINFORCED COMPOSITE T-JOINTS: A FINITE ELEMENTS SIMULATION

G. Allegri, X. Zhang

Aerospace Engineering Group, School of Engineering, Cranfield University, Bedford MK43 0AL, UK

ABSTRACT

This paper addresses the damage tolerance capability of laminated T-joints having through-thickness reinforcement by Z-fibres. This kind of reinforcement, usually referred to as Z-pinning, has been developed by Foster-Miller and Aztex in the USA since 1992, to improve the damage tolerance of traditional laminated composites. A 3D FE model of a composite T-joint has been developed. The model represents delamination and debond in the web-to-base bonded flange by a proper combination of linear and nonlinear spring elements; the latter describes the bridging forces exerted by Z-pins during the delamination growth. The modelling strategy has been validated by means of experimental data regarding both unpinned and pinned composite T-joints.

1. INTRODUCTION

The assembly of large composite structures requires design and manufacturing of proper joining members, which can be either mechanically fastened or adhesively bonded. Usually bonded joints allow for higher damage tolerance performances for the whole structure, since the continuity of the reinforcement fibres is not broken by fastening holes, thus avoiding local high stress concentrations. However, bonded joints are susceptible to out-of-plane stresses.

Among the wide range of geometrical configurations suitable for manufacturing composite structural joints, the T layout is one of the simplest, yet providing an easy way to transfer out-of-plane loads. T-joints are commonly employed in the aerospace field to manufacture wing stiffener-to-skin interfaces, fuselage bulkhead-to-skin connections and spar-to-skin interfaces. Moreover similar applications are common in the naval and automotive fields. Techniques to manufacture T-joints include conventional lay-up of C channels with radius fillers and reinforcing caps [1] and resin transfer moulding of three-dimensional woven fabric preforms [2].

The methods described are suitable for assembling large composite structures by T joints, yet obtaining proper damage tolerance performances for adhesively bonded composite joints still represents an open problem, especially for the conventional lay-up techniques [3]. The out-of-plane load transferring capability of the T-joint is also responsible for the mixed-mode delamination growth in the web-to-base flange [4]; the damage evolution pattern under static and cyclic loading is related to several factors, involving both the joint configuration and the applied forces [5]. Nevertheless, the final failure of the T-joint is always dependent on the loss of load bearing capability due to delamination growth [6]. Delamination growth in bonded joints is usually initiated by pre-existing small flaws under both static and fatigue loading. Thermal cycling and moisture absorption may also contribute to the damage development.

Several papers have addressed methodologies to model delamination growth in adhesively bonded joints. The first conclusion which can be drawn is that a fracture mechanics approach is suitable to describe delamination growth [7-8] under quasi-static loading; this modelling approach is based on FE analysis of bonded joints and usually involves computing the strain energy release rate (SERR) at the delamination tips and FE model updating if the Griffith's local failure criterion is satisfied. This method has been successfully applied to the failure analysis of adhesively bonded T-joints [9] and it is well suited to also cope with fatigue loading and environmental effects [10].

The main differences among the analyses presented in the literature are mainly related to the mathematical formulation of the finite elements employed, the techniques for evaluating interfacial stresses between composite laminate plies, and finally the geometric and loading configurations of the T-joints studied. Theotokoglou [11-12] investigated both experimentally and numerically the ultimate strength of sandwich T-joints under pull-off loading.

Delamination growth has been modelled by means of a nonlinear FE analysis in 2D plane strain conditions. Hoyt et al. [13] investigated the static strength, crack growth and fatigue life of a stiffener-to-skin T joint belonging to a rotorcraft composite structure; the structure itself was assumed to operate in a post-buckling stage, when high interlaminar shear and peeling stresses occur in the T-joints subjected to compressive loading. The analysis was carried out by means of a 2D plane strain nonlinear FE analysis. Damage initiation is predicted through a materials strength criterion and delamination growth is modelled by a fracture mechanics approach by calculating the SERR at the delamination tips. According to this analysis, when applying a compressive load on the web, delaminations occur at the bond-line between the T-joint tapered flange and the supporting skin, growing from the tips of the flange towards the middle section of the joint.

The insertion of a through thickness reinforcement in the most stressed regions of a T-joint can strongly improve its static strength performance and damage tolerance capabilities, thus stitching has been widely employed in the past to prevent delamination growth in the T joint web-to-base flange. Tada and Ishikawa [14] investigated the damage tolerance of stitched T-joints under compressive loading, finding that through thickness reinforcement can stop the delamination growth and increase the ultimate strength. Young and Chuang [15] evaluated the ultimate strength of both unstitched and stitched composite T-joints under tensile loading; the results proved a substantial increase of the joint tensile strength. Rispler et al. [16] developed an FE analysis of the T-joints and showed that delaminations initiated in the web-to-flange radius filler, due to matrix cracking. Stickler et al. [17-18] investigated the mechanical response of stitched composite T-joints under pull-off, shear and flexural loading: FE analyses, validated by experimental results, were performed in order to estimate the damage initiation load for various combinations of the tow modulus and fibre insertion depth, providing general design guidelines.

An alternative technique providing an efficient through-thickness reinforcement for composite laminates is Z-pinning, which has been established more recently compared to stitching for industrial applications [19]. Z-pinning was shown to be an economically feasible and reliable technique to improve the damage tolerance of composite structures, especially regarding delaminations arrest [20]. Z-pins insertion slightly affects the in-plane mechanical properties of composite laminates, mainly depending on pin diameter and volumetric fraction. A 10% to 15% loss of in-plane mechanical properties is expected for pinned laminates, while the out-of-plane stiffness is generally increased by 25% [21]: the loss of in-plane elastic properties is remotely dependant on the laminate stacking sequence. The experimental and numerical investigation [22] of the behaviour of Z-pinned DCB specimens has clearly shown the highly beneficial effect of this through-thickness reinforcement technique on the CFRP damage tolerance in mode I loading: though delamination initiation is not prevented, their growth is much delayed, due to the fact the Z-pins are able to absorb a large amount of elastic energy, especially during their pull-out stage. Therefore the apparent out-of-plane toughness of Z-pinned laminates is strongly enhanced, depending on Z-pin volumetric density and diameter. The best damage tolerance performances are achieved for a pin volumetric density ranging between 2% and 4% and a diameter about 0.25 mm: employing Z-pins with a bigger radius is only slightly beneficial for damage tolerance and the loss of in-plane mechanical properties can be severe, also leading to in-plane crack growth. Moreover, an increase of the volumetric fraction of Z-pins above the aforementioned values leads to a rise in the manufacturing cost and complicates the insertion process.

This work investigates the effect of Z-pinning on T-joints under pull-off loading. A detailed 3D FE model of the T-joint has been developed: the flange to base-skin interface has been modelled by a set of discrete springs representing the peel and shear elastic response of the adhesive bond. Delamination growth has been simulated by means of the Virtual Crack Closure Technique (VCCT), modelling the Z-pins as nonlinear springs, behaving according to an analytical constitutive law validated by experimental data. The effects of various pin

volumetric densities and diameters have been investigated. The numerical results have been validated through experimental tests.

2. PROBLEM STATEMENT

The geometry of the T-joint analysed is sketched in fig. 1. The joint was manufactured by means of conventional lay-up, employing the Hexcel G986/M36 carbon/epoxy fabric prepreg, whose mechanical properties are reported in Table 1. This material was chosen since it has a high fracture toughness, both in mode I and mode II.

The supporting base of the joint was made of 8 prepreg layers, each 0.28 mm thick, with $[0/(45)_2/(0)_5]$ orientation, resulting in a total thickness t_S = 2.24 mm. The flange was manufactured employing a 10-ply laminate $[45/(0)_2/(45)_2/(0)_5]$ of the aforementioned prepreg, having a total thickness t_f = 2.8 mm. Finally the web was made of a $[0,45]_S$ carbon fabric laminate, whose total thickness is t_w = 1.12 mm. The supported length of the T-joint is L = 80mm, while the total height is H = 40 mm. The width of the joint was W = 40 mm.

Ending tabs were added to the web to provide a proper redistribution of the load applied by the gigs. The central core radius of the T-joint was reinforced by insertion of a composite filling noodle, still made of G986/M36 carbon fabric. The web-to-base flange was reinforced by insertion of T300/BMI Z-Fiber™ pins, employing an ultrasonic gun [23]. The fibres diameter and volumetric density varied for different samples.

The T-joints have been tested by applying a quasi-static tensile load up to the final failure and registering the gigs displacements. The failure of the joint is due to delamination growth both in the web-to-base flange and in the web: this observation has been confirmed by both photographic recording of the delaminations progress and post-failure investigations.

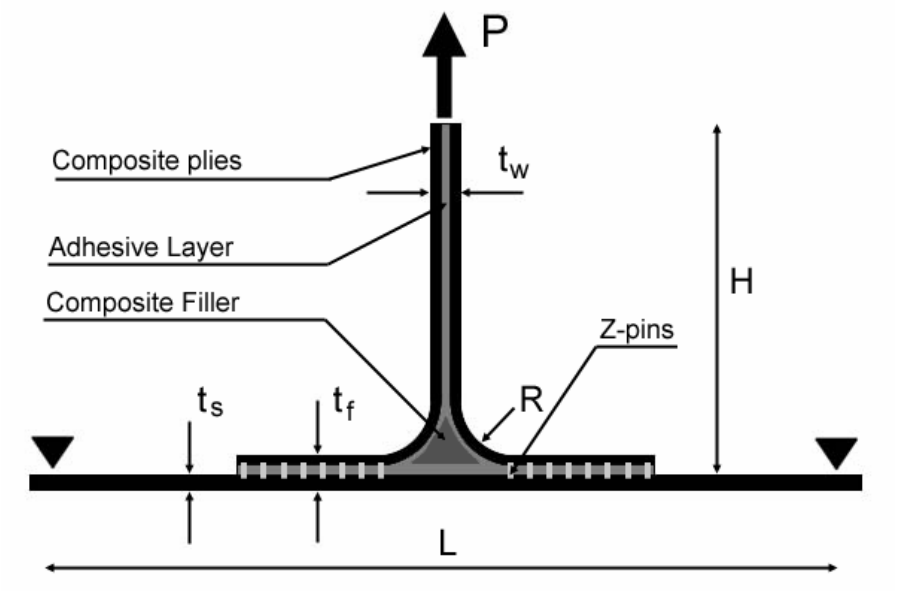

"**Fig. 1**: T-Joint geometry: front view"

Material	E_1 (GPa)	E_2 (GPa)	G_{12} (GPa)	ν_{12}	X_t (MPa)	X_c (MPa)	Y_t (MPa)	Y_c (MPa)	ILSS (MPa)
M36/G986	67	67	14	0.05	855	600	855	600	71
M36	3.5	3.5	1.3	0.33	81	146	81	146	
Z-Fiber™	115								

"**Table 1**: materials mechanical properties"

3. T-JOINT BEAM MODEL

A simplified beam model of the T-joint has been developed to get some insight on the stress distribution which affects the structure, particularly regarding the initiation and growth of delaminations. As clearly shown in fig. 1, the joint itself is symmetric, thus only one half of the structure needs to be considered, providing that proper symmetry constraints are applied.
The joint beam model is sketched in fig. 2: the geometric and load symmetry in the central section has been accounted for by inserting sliding constraints to the ends A and B, which prevent x displacement and z rotation, while the end D is simply supported. The bending stiffness of each beam segment is represented by lines having different thicknesses. The length L_1 and L_2 represent delamination sizes in the web and base flange, respectively.

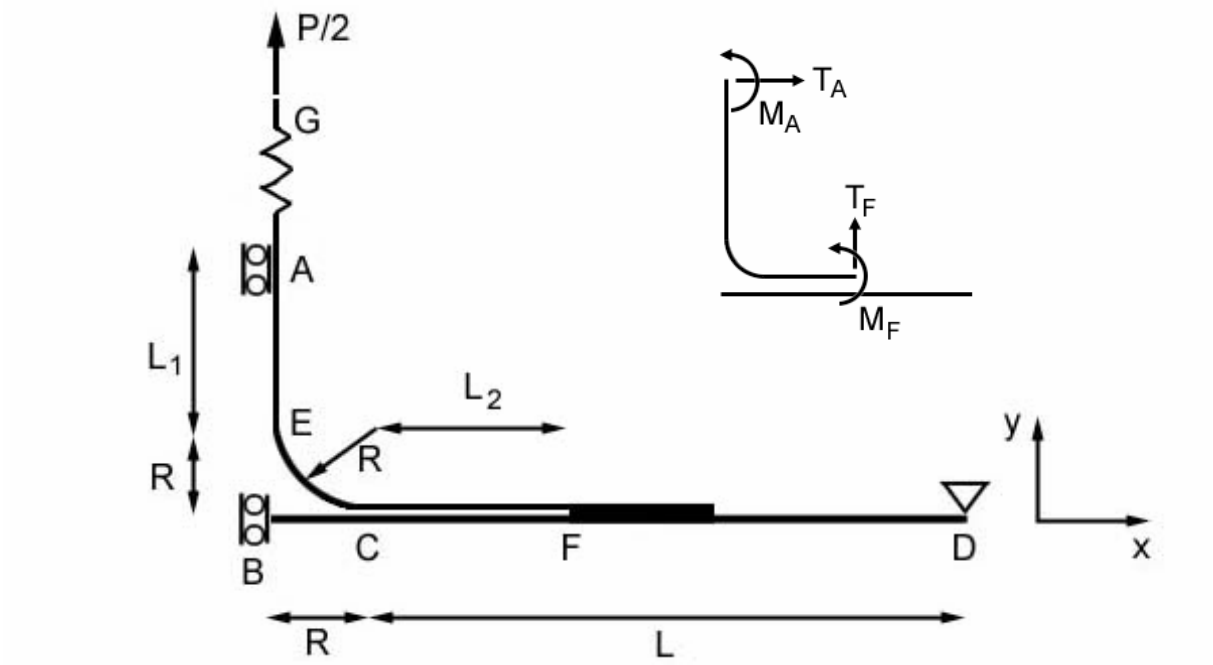

"**Fig. 2**: T-Joint beam model"

The structure shown in fig. 2, representing one half of the joint, is twice hyper-static; the equivalent iso-static system can be easily obtained by substituting the sliding constraint at point B by its unknown reaction force and torque.

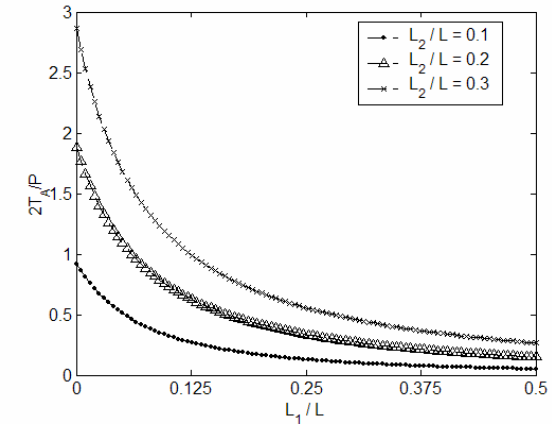

"**Fig. 3**: constraint shear at point A"

Assuming that the beam deformation is only due to bending moments and applying the classical force method together with the virtual work principle, it is easy to evaluate the bending moment and shear force acting on the delamination tips A and F (see the insertion in fig. 2). The results of this analysis are presented in figs 3, 4 and 5.
The forces are assumed positive if directed as the axis in fig. 2; anticlockwise moments are positive. The shear force acting at point F (fig. 2) is y-directed, always positive and equal to half of the total load P. On the other hand, the shear force at point A and the moments at points A and F are dependent on the relative magnitude of the delamination lengths. As shown in fig. 3, the shear at point A, which is oriented as the x-axis, is always positive for any combinations of the delamination growth: the resulting shear represents a mode I opening force acting at the tip of the web delamination, whose magnitude can be

highly magnified if compared to the applied load. Therefore fig. 3 shows that, if a delamination grows in the web-to-base flange, a high shear force will arise in the web, leading to the propagation of a y running crack. The longer the delamination in the web-to-base flange, the higher the shear force acting on the web; the shorter the crack in the web, the higher the resulting shear at the delamination tip. If the crack in the web grows, the local shear magnitude decreases sensibly; nevertheless the shear at the flange delamination tip, thus the mode I opening force for that crack, is always dependent only on the applied load P.

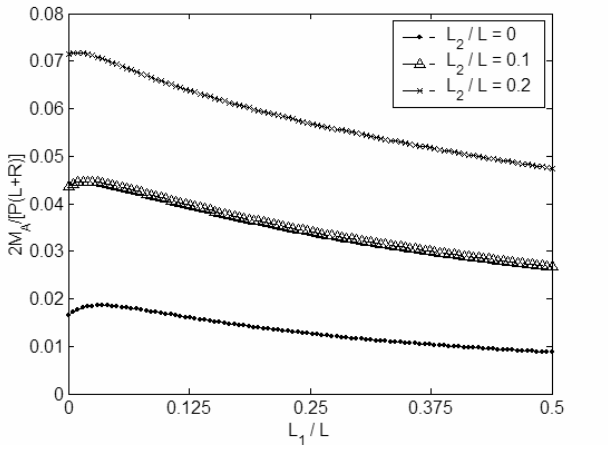

"**Fig. 4**: constraint bending torque at point A"

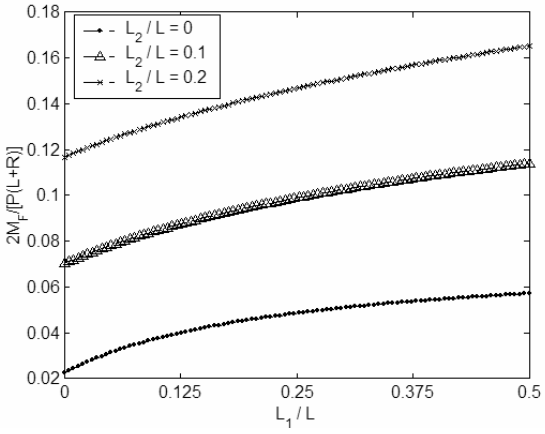

"**Fig. 5**: constraint bending torque at point F"

As shown in fig. 4, the beam moment acting at point A is always anticlockwise, therefore it contributes to the mode I web crack growth; similar to the shear, the longer the delamination in the web-to-base flange, the higher the torque acting on the web crack tip. In contrast, since the torque acting at point F is anticlockwise as shown in fig. 5, it tends to close the flange delamination, thus retarding its propagation. The bending torque in F increases with the lengths of both the web and flange delaminations, therefore the crack closing effect tends to be stronger with the damage growth.

Summarising the previous considerations, we can conclude that a delamination in the web can initiate and grow quickly if a crack is present in the web-to-base flange, due to a redistribution of the bending torque and shear over the whole structure. In contrast, the mode I opening of web-to-flange is positively influenced by the presence of a crack in the web, since the local bending torque tends to close the delamination, while the mode I crack opening force, i.e. the local resulting bending shear, depends only on the tensile load applied.

4. T-JOINT FE MODEL

A numerical procedure has been established to simulate the delaminations growth in the T-joint considered. A detailed 3D FE model of the T-joint has been developed and processed by NASTRAN: laminate shell 4-noded (CQUAD4) elements have been employed to model the CFRP static response under increasing load.

Only one quarter of the T-joint has been meshed, due to its x and z symmetries; proper constraints have been applied to simulate the supporting boundary conditions and the aforementioned symmetries. Spring (CELAS2) "interface" elements have been introduced in the model to simulate the peel and shear response of the adhesive layer [24] according to the mechanical properties presented in tab. 1. The spring "interface" elements perform as elastic connections between the two sub-laminates which are going to be separated during the delamination growth. The elements in the flange-to-base overlapping are square, having an area of $1mm^2$.

The FEM model of the T-joint is shown in fig. 6. The clamp action has been modelled by means of a set of rigid elements, connecting the upper end of the web laminate to a reference node where a concentrated external load has been applied.

A set of MATLAB subroutines have been written to manage the simulation of the delamination initiation and growth processes: these subroutines perform a post-processing analysis of the results, acquiring the values of the spring axial forces and calculating the peel and shear stresses within the adhesive layer. The damage initiation is predicted by the following criterion

$$\left(\frac{\sigma_z}{\sigma_u}\right)^2 + \left(\frac{\tau}{\tau_u}\right)^2 \geq 1 \qquad (1)$$

where σ_z is the peel stress, τ is the in-plane shear stress, σ_u and τ_u are the adhesive ultimate peel and shear strengths. If the strength based failure criterion in (1) is satisfied for an arbitrary set of spring elements, these latter are automatically deleted from the model, thus creating initial flaws.

After the delamination initiation, the following crack growth process is modelled by a fracture mechanics approach: the SERR at the delamination tips is calculated by means of the VCCT [25] and the crack growth is modelled employing the following criterion

$$\frac{G_I}{G_{Ic}} + \frac{G_{II}}{G_{IIc}} \geq 1 \qquad (2)$$

where G_I and G_{II} are the strain energy release rates, respectively in mode I and mode II, while G_{Ic} and G_{IIc} are the corresponding critical values. As in the case of the strength-based criterion in eq. (1), if eq. (2) is satisfied for a set of springs, these latter are removed from the model.

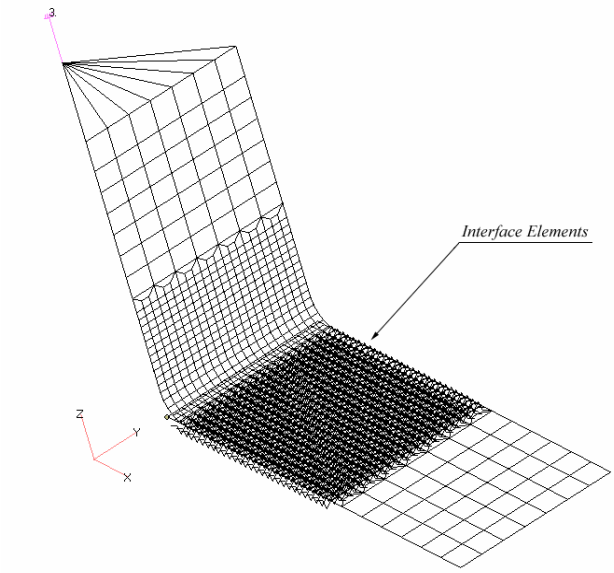

"**Fig. 6**: T-joint FE model"

If the T-joint is reinforced by the insertion of Z-pins, after the adhesive local failure the linear springs are substituted by 1D nonlinear elements (PBUSH1D), whose load-displacement response represents the pin behaviour during progressive debonding and pull-out.

The constitutive model of carbon fibre Z-pins employed in the simulations has been developed by the authors [26], which is fully analytical and it is hinged on describing of the pin as a beam on an elastic foundation, having both axial and bending compliance. The key-parameter to predict the load-displacement response of a single pin is represented by the frictional sliding shear t, whose value depends on the pin diameter and on the laminate elastic properties. The value of the Z-pin sliding shear t can be experimentally assessed by either mode I or mode II single pin pull-out tests: nevertheless in the present study the value of the pin frictional sliding shear t has been estimated by calibrating the constitutive model in order to fit the T-joint experimental load-displacement response with the FE analysis results.

The FE simulation of the T-joint tensile response is displacement-controlled: once the delaminations initiates, iterative static analyses are performed at constant external loading, updating the delamination geometry until the crack front reaches a stable configuration. In this condition the load and displacement values are saved and the analysis goes on increasing the external load by a prescribed fixed step. The simulation ends when the flange is completely detached from the supporting base.

5. RESULTS AND DISCUSSION

The FE simulation of the T-joint response under increasing quasi-static tensile loading has been performed by considering four different test cases:

1. unpinned T-joint (control case);
2. Z-pinned, with 0.28 mm fibre diameter and 2% volumetric density;
3. Z-pinned, with 0.28 mm fibre diameter and 4% volumetric density;
4. Z pinned, with 0.5 fibre diameter and 2% volumetric density.

5.1 Unpinned T-Joint

The analysis of the unpinned T-joint is crucial to understand the effect of the delamination in the web on the crack growth between the flange and the supporting base. The critical values of the mode I and mode II SERR have been evaluated by means of DCB and MMB tests on the G986/M36 composite, yielding G_{Ic} = 1250 J/m^2, G_{IIc} = 1100 J/m^2 [27]. It is worth to observe that the composite employed to manufacture the T-joint is considerably tougher than other commercially available CFRP.

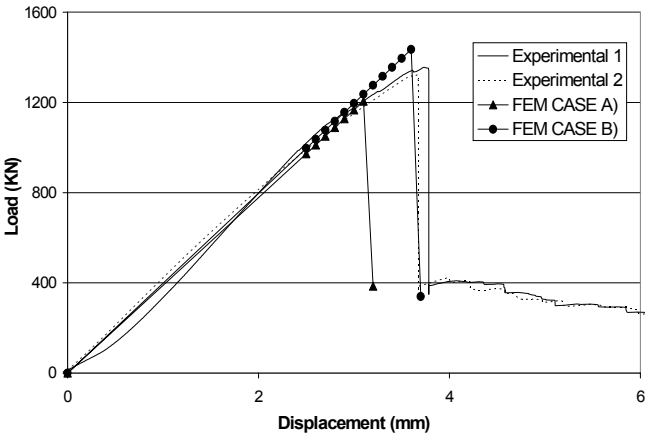

"**Fig. 7**: results for the unpinned T-joint"

The simulation results are summarised in fig. 7. Strictly speaking, a rigorous simulation of the delamination growth within the web would have been necessary. However the presence of a crack in the web for the T-joint configuration here discussed mainly depends on the very low thickness of the web itself; therefore it can be easily avoided in practical circumstances, by simply thickening the web laminate with additional plies. The key of the structural problem is still the flange-to-base delamination growth, which limits the T-joint capability of transferring out-of-plane loads. Moreover the beam analytical model of the T-joint discussed in Sec. 3 has pointed out that the crack opening force for the web delamination is strongly magnified if compared to the applied load, especially for short flange-to-base delamination lengths. Therefore it has been assumed that the crack in the web grows much more quickly than that in the horizontal flange; thus, for application purposes, we can state that the crack in the web is always present and that it has an almost constant length. This hypothesis is confirmed by visual observations of the crack tip positions during the experimental tests. Two different scenarios have been considered for the web delamination length: case A), for which the web defect size is 5mm, and case B), the defect size being 10 mm. From the FE results shown in fig. 7, we can observe that the T-joint stiffness variation for the two scenarios is negligible, but for a web delamination 5 mm long the joint failure load and displacement are strongly underestimated. This result is consistent with the beam analysis of the T-joint, which has pointed out that a crack closing torque acts on the flange delamination tip; the torque magnitude increases with the web delamination length, thus a longer crack in the web tends to delay the flange-to-base delamination growth.
The post-processing analysis of the SERR distributions at the crack tips points out that the delamination growth occurs in almost pure mode I.
In fact, increasing the web crack size up to 10mm, case B), yields FE results which agree well with experimental ones. Therefore the FE simulations for the Z-pinned T-joints have been performed by placing a 10mm long delamination in the web.

5.2 Z-pinned T-joint,0.28 mm diameter, 2% volumetric density

The insertion of Z-pins in the T-joint requires to model the nonlinear behaviour of the through thickness reinforcement; this means that every analysis step involves either the delamination front update or the load increment becomes nonlinear, thus demanding a longer computational time. The frictional sliding shear t in the pin constitutive model must be assessed calibrating the FE model results with the experimental data: the higher the frictional sliding shear, the slower flange-to-base delamination growth.

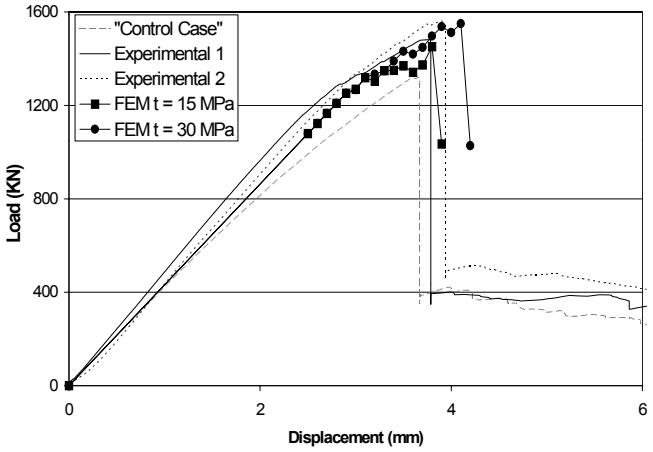

"**Fig. 8**: results for the 0.28mm, 2% pinned T-joint"

The results of the analysis are shown in fig. 8. The FE analysis underestimates the experimental load-displacement response for a frictional sliding shear of 15 MPa. A satisfactory agreement is achieved by increasing the pull-out friction up to 30 MPa.

Adding a 2% volumetric fraction of 0.28mm diameter Z-pins increases the maximum bearable load by about 8%, and the failure displacements is increased by 5%. According the FE analysis the pin insertion has very little effect on the damage initiations, which occurs at about 1260N, (2.9 mm in terms of displacement). In contrast to the behaviour of the unpinned T-joint, the pinned joint is more damage tolerant, though the beneficial effect is still quite small.

5.3 Z-pinned T-joint,0.28 mm diameter, 4% volumetric density

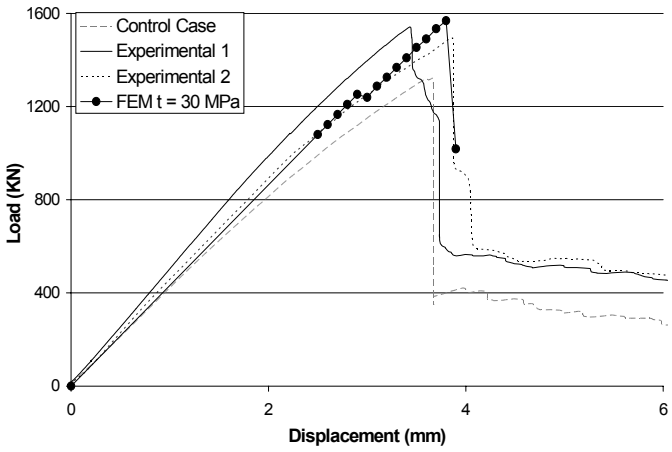

"**Fig. 9**: results for the 0.28mm, 4% pinned T-joint"

Increasing the volumetric density of the through thickness reinforcement allows to absorb a larger amount of elastic energy by the Z-pins, thus reducing the energy quota available to create new fracture surfaces and make the crack grow. The analysis results are shown in fig. 9. In this case the through thickness reinforcement proves to be very efficient in delaying the flange-to-base delamination growth: both the T-joint maximum bearable load and failure displacement are now increased by about 10%. The FE analysis shows only a small delamination propagation after the initiation, which once again occurs at the same load level found for the unpinned T-joint; the failure is less progressive than for the previously considered pinned configuration, but it occurs at higher loads and displacements.

5.4 Z-pinned T-joint,0.5 mm diameter, 2% volumetric density

From a physical point of view, increasing the pin radius is almost equivalent to raise the frictional sliding shear t. This occurs because the insertion of a larger pin in the laminate provides a larger displacement for the surrounding fibres, which react by applying a larger residual force on the pin itself. On the other hand a sensible loss of in-plane mechanical properties should be expected, due to the local misalignment of the laminate fabric.

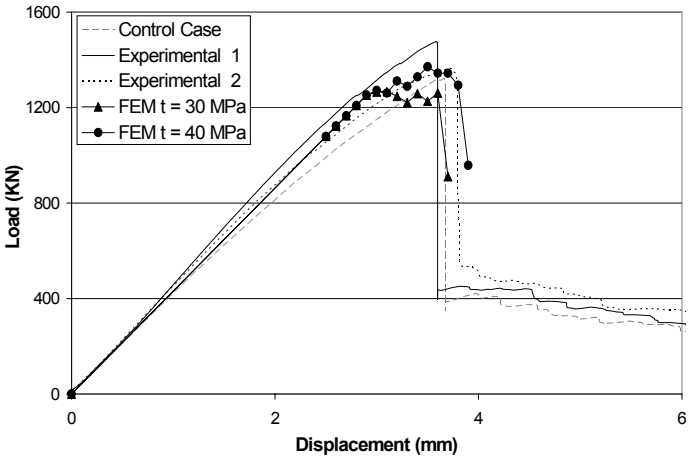

"**Fig. 10**: results for the 0.5mm, 2% pinned T-joint"

For this T-joint configuration this effect is mitigated by the gain in out-of-plane stiffness which the insertion of pins usually provides, since the applied tensile load can be resisted also by the out-of-plane deformation of the flange. In the case of the T-joint here modelled, the two aforementioned effects are almost comparable, so the insertion of Z-pins does not change the slope of the load-displacements curves for the different configurations examined.

A good agreement between FE results and experimental ones is now obtained by increasing the frictional sliding shear up to 40 MPa, in order to take into account the larger pin diameter. The resulting effect on the T-joint load-displacement curve is close but somewhat below that achieved by adding 2% of 0.28mm diameter pins. This result is not surprising, since the local forces exerted by the pins are now smeared over a larger area, due to the fact that the distance between two adjacent pins is a linear decreasing function of the Z reinforcement diameter if the volumetric fraction is kept constant.

6. CONCLUSION

Z-pinning is a well established industrial process to provide an efficient through thickness reinforcement of traditional composite laminates. In spite of its relatively wide employment in the aerospace, automotive and naval fields, modelling the mechanical response of Z-pinned composites still requires deep investigations, particularly regarding the through thickness reinforcement capability of either delaying or suppressing delamination growth.

The quasi-static mechanical response of a composite T-joint subjected to an increasing tensile load has been considered as a benchmark problem to validate a numerical technique to simulate the delamination progression in Z-pinned structural joints. This work is based on the FE analysis of the structural joint, combined with a post-processing step focused on the SERR computation at the delamination tips. Linear elastic fracture mechanics is applied using the VCCT to evaluate the delamination progression pattern in structural joints under general mixed mode conditions. This simulation method has been implemented in the MATLAB environment, employing NASTRAN as main processor for the FE analysis. The method implementation also comprehends a constitutive model of the Z-pin response, developed by the authors.

The FE simulations results show a satisfactory agreement with the experimental load-displacements curves for the T-joint configuration examined: the insertion of Z-pins within the web-to-base flange of the joint improves significantly the damage tolerance capabilities, increasing both the maximum static operative load and the failure pull-off displacement. The effects of variable z-fibre volumetric densities and diameters are correctly predicted.

ACKNOWLEDGEMENTS

The work was funded by the DTI CARAD program via the JOINTS project. The authors wish to thank Drs. I.K. Partridge, D. Cartié and M. Troulis for providing validation experimental data.

References

1. **Baker A.**, "Joining and repair of aircraft composite structures", *In: Mallick, P.K., editor. Composite Materials Handbook, New York: Marcel Decker,* (1997).
2. **Soden, J.A.**, **Weissenbach**, **G.**, and **Hill**, **B. J.**, "The design and fabrication of 3D multi-layer woven T-section reinforcements", *Compos. Part A: Appl. Sci. Manufact.*, ***30***, (1999), 213-20.
3. **Charalambides, M.N.**, et al., "Strength prediction of bonded joints*", 83rd Meeting of the AGARD SMP-Bolted/Bonded Joints in Polymeric Composites*, (1997).
4. **Minguet**, **P.J.**, "Analysis of the strength of the interface between frame and skin in a bonded composite fuselage panel", *Proceedings 38th AIAA Structures, Structural Dynamics and Materials Conference,* (1997).
5. **Pradhan**, **S.C.**, **Iyengar**, **N.G.R** and **Kishore**, **N.N.**, "Parametric study of interfacial debonding in adhesively bonded composite joints", *Compos. Struct.*, ***29(1)***, (1994), 119-25.
6. **Cvitkovich**, **M.**, **O'Brien**, **T.K.** and **Minguet**, **P.J.**, "Fatigue debonding characterization in composite skin/stringer configurations", *NASA Tech Memo 110331/Army Research Lab Report 1342*, (1997).
7. **Johnson**, **W.S.**, et al., "Application of Fracture Mechanics to the durability of bonded composite joints", *FAA Final Report DOT/FAA/AR-97/56*, (1988).
8. **Minguet**, **P.J.**, and **O'Brien**, **T.K.**, "Analysis of skin/stringer bond failure using a strain energy rate approach", *Proceedings of the Tenth International Conference on Composite Materials (ICCM-X)*, Vancouver, British Columbia, Canada, (1995).
9. **Theotokoglou**, **E.E.**, and **Moan**, **T.**, "Experimental and numerical study of composite T-joint", *J. Compos. Mater.*, **30**(2), (1996), 190-209.
10. **Fernlund, G.**, et al., "Fracture load predictions for adhesive joints", *Compos. Sci. Tech..*, ***51***, (1994), 587-600.
11. **Theotokoglou**, **E.E.**, "Study of numerical fracture mechanics analysis of composite T-joints", *J. Reinforced Plastics Compos.*, **18**(3), (1999), 215-23.
12. **Theotokoglou**, **E.E.**, "Study of composite T-joints under pull-off loads", *J. Reinforced Plastics Compos.*, **16**(6), (1999), 503-518.
13. **Hoyt**, **D.M.**, **Ward**, **S.H.**, and **Minguet**, **P.J.**, "Strength and fatigue life modelling of bonded joints in composite structures", *J. Compos. Tech. Res.*, **24**(3), , (2002), 188-208.
14. **Tada**, **Y.**, and **Ishikawa**, **T.**, "Experimental evaluation of the effects of stitching on CFRP laminate specimens with various shapes and loading", *Key Eng. Mater.*, **37**, (1989), 305-16.
15. **Young**, **W**. **B.**, and **Chuang**, **M.T.**, "Fabrication of T-shaped composite through resin transfer moulding", *J. Compos. Mater.*, **29**(16), (1996), 2192-214.
16. **Rispler**, **A.R.**, **Stevens**, **G.P.**, and **Tong**, **L.**, "Failure analysis of composite T-joints including inserts", *J. Reinforced Plastics Compos.*, **16**(18), (1997), 1642-58.
17. **Stickler**, **P.B.**, **Ramulu**, **M.**, and **Johnson**, **P.S.**, "Experimental and numerical analysis of transverse stitched T-joints in bending", *Compos. Struct.*, **50***,* (2000), 17-27.
18. **Stickler**, **P.B.** and **Ramulu**, **M.**, "Parametric analyses of stiched composite T-joints by the finite element method", *Materials & Design*, **23**, (2002), 751-58.
19. **Freitas**, **G.**, **Fusco**, **T.**, **Magee**, **C.**, and **Dardzinski P.**, "Fiber insertion process for improved damage tolerance in aircraft structures", *J. Adv. Mater.*, **25**, (1994).
20. **Cartie**, **D.D.R.**, and **Partridge**, **I.K.**, "Z-pinned composite laminates: improvements in delaminations reistance", *Proceedings of the Fifth International Conference on Deformation and Fracture in Composites*, (1999).
21. **Grassi**, **M.**, **Zhang**, **X.**, and **Meo**, **M.**, "Prediction of stiffness and stresses in Z-fibre reinforced composite laminates", *Compos. Part A: Appl. Sci. Manufact.*, ***33***, (2002), 1653-64.
22. **Grassi**, **M.**, and **Zhang**, **X.**, "Finite element analysis of mode I interlaminar delaminations in Z-fibre reinforced composite laminates", *Compos. Sci. Tech.*, **63**, (2003), 1815-32.
23. **Troulis**, **M.**, **Cartie**, **D.D.R.**, **Barattoni**, **L.**, and **Partridge**, **I.K.**, "Z-pinned woven laminates: interlaminar fracture results and pinned quality considerations", *Proceedings of the Sixth International Conference on Deformation and Fracture of Composites (DCF 6)*, Manchester, (2001).
24. **Wu**, **G.**, and **Crocombe**, **A.D.**, "Simplified finite element modelling of structural adhesive joints", *Comput. Struct,,* **61**, (1996), 385-91.
25. **Krueger**, **R.**, "The Virtual Crack Closure Technique: history, approach and applications", *NASA/CR-2002-211628*, *ICASE Report No. 2002-10,* (2002).
26. **Zhang**, **X.** and **Allegri**, **G.**, "JOINTS Project Internal Report", *Cranfield University*, February (2004).
27. **Troulis**, **M.**, Ph.D. Thesis, *Cranfield University,* March (2004).